Deformation of Drops in Extensional Viscoelastic Flow

R. GONZALEZ-NUNEZ,[1] C. F. CHAN MAN FONG,[2] B. D. FAVIS,[3] and D. DE KEE[2,*]

[1]Facultad de Ciencias Quimicas, Universidad de Guadalajara, Mexico, [2]Department of Chemical Engineering, University of Sherbrooke, Sherbrooke, Quebec J1K 2R1, Canada, and [3]Department of Chemical Engineering, Ecole Polytechnique-Montreal, Canada

SYNOPSIS

The deformation of nylon drops in polyethylene, with and without an interfacial agent, in an extensional flow has been studied. The presence of an interfacial agent reduces the size of the dispersed phase, and the deformation of the drop is reduced. An analysis is given, which accurately predicts the deformation for all values of the capillary number considered. The predicted and observed shapes are, however, only in agreement at low values of capillary number. Possible causes for this discrepancy are discussed. © 1996 John Wiley & Sons, Inc.

INTRODUCTION

The physical blending of two or more polymers resulting in a new product with desired properties is of great industrial importance.[1] From a rheological viewpoint, polymer blends can be considered to be dispersions of deformable polymeric drops in polymer melts. The mechanical properties of the blends depend on the state of the dispersion; that is, they depend on the shape, size, and orientation of the dispersed phase. It has been found that the addition of interfacial agents can improve the properties of blends of immiscible polymers.[2-4]

Taylor[5] initiated the study of the deformation of a drop in a Newtonian fluid. Since then, numerous investigators[6-11] have considered drops in Newtonian and non-Newtonian fluids. Rallison[12] and, more recently, Stone[13] have reviewed the major contributions in this area. Tsebrenko et al.[14] have summarized the experimental results of the deformation and breakup of polymeric particles in mixtures of immiscible polymers in various flow situations. Also relevant to the present work are the studies of Milliken et al.[15] and Milliken and Leal[16] on the effects of surfactants on drop deformation in various flow situations. Many of the previous authors have considered the deformation of a drop in a shear flow and in a planar extensional flow. In many industrial applications, the flow is a uniaxial elongational flow, and it is desirable to consider the drop deformation in such a flow.

In the present paper, we examine the deformation of drops of nylon-6 in polyethylene in a uniaxial extensional flow. The effects of the presence of an interfacial modifier is also considered.

EXPERIMENTS

Four kinds of commercial polyethylene 07055C (PE1), 05054C (PE2), and 36056 (PE3) from Dow and 2914 (PE4) from DuPont are used as the matrix. The minor phase is nylon-6 (PA6) Zytel from DuPont. In some cases, Surlyn 9020 from DuPont is added as an interfacial agent. This ionomer is a random terpolymer consisting of approximately 80% PE and of 20% of a mixture of methacrylic acid and isobutyl acrylate. The methacrylic acid is approximately 70% neutralized with zinc. Willis et al.[17] have shown that this ionomer is an excellent compatibilizing agent for PA/PE systems.

Covalent bonding was shown to take place between the carbonyl of the ionomer and the terminal amine of the polyamide.[18] The melt densities at 250°C of PE, PA6, and ionomer are 0.74, 0.96, and 0.74 g/mL, respectively.

The mixture is prepared in a twin screw extruder (ZSK-30 Werner-Pfeiderer), and the blend is then extruded through a single screw Brabender-type extruder with a rectangular slit. The extruded tem-

* To whom correspondence should be addressed.

Journal of Applied Polymer Science, Vol. 62, 1627-1634 (1996)
 CCC 0021-8995/96/101627-08

perature is 250°C. The rectangular sheet is then taken up on a roll, which is water-cooled. The experimental setup is shown in Figure 1. The take-up velocity V_R at the roll is greater than the extrusion velocity V_E, and the flow can be considered to be an extensional flow. The area A_O, the thickness h_O, and the velocity V_E at the exit of the extruder are 3.567 $\times 10^{-5}$ m^2, 1.524 $\times 10^{-3}$ m, 6.5 $\times 10^{-3}$ m/s, respectively.

The length L and the half width W of the sheet are 1.2 $\times 10^{-1}$ and 2.341 $\times 10^{-2}$ m, respectively.

The rheological properties of the materials are determined using a Bohlin CS rheometer, a parallel plate Weissenberg rheometer, and an Instron capillary rheometer. Figure 2 shows the viscosity $\eta(\dot{\gamma})$ and the dynamic viscosity $|\eta^*(\omega)|$ of some of the polymers.

A scanning electron microscope (JOEL 35 CF) is used to analyze the size and shape of the dispersed phase. A Jandel digitizing tablet controlled by the Jandel Sigma-Scan system is used to measure the size and shape of the dispersed phase. About 200 droplet diameters are measured, and a correction is applied to the distribution of diameters for each sample according to the method given by Saltikov.[19] The required samples are prepared in liquid nitrogen, following the mixing and spinning steps.

In the die, the flow is a shear flow, and an initially spherical drop deforms into an ellipsoid and orients itself at an angle to the direction of the flow. At low shear stress [Fig. 3(a)], there is no significant deformation, and the dispersed phase can be assumed

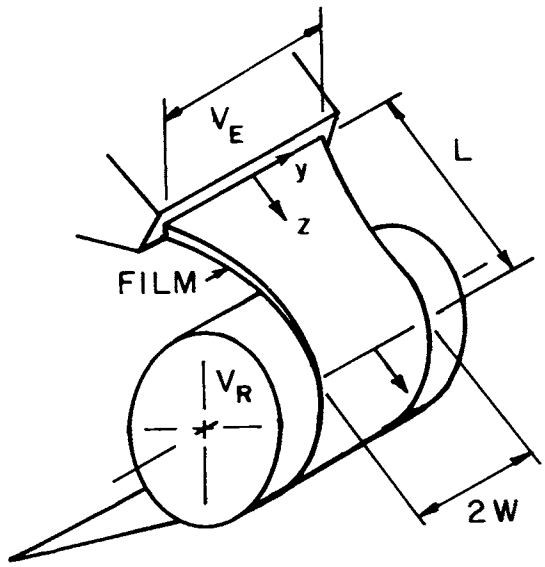

Figure 1 Extrusion of a plane sheet.

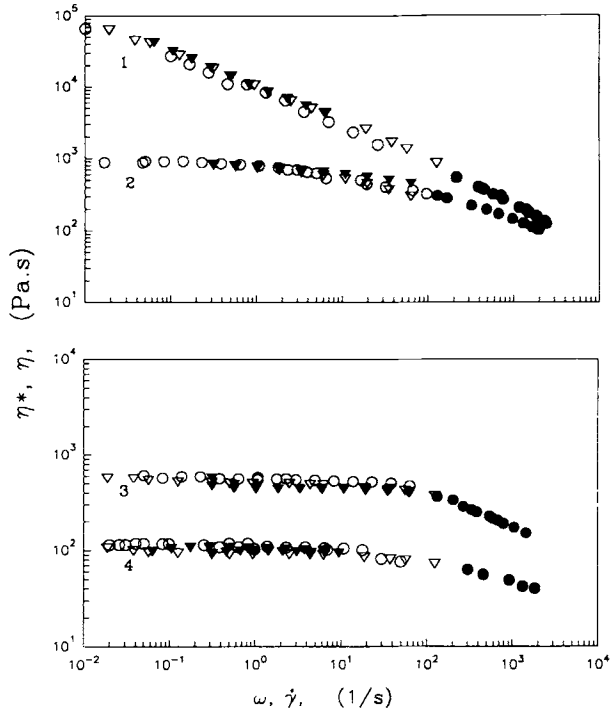

Figure 2 Viscosity $\eta(\dot{\gamma})$ versus shear rate $\dot{\gamma}$, and dynamic viscosity $|\eta^*(\omega)|$ versus frequency ω: (▼) $|\eta^*(\omega)|$ Bohlin CS, (▽) $|\eta^*(\omega)|$ Weissenberg, (○) $\eta(\dot{\gamma})$ Weissenberg, and (●) $\eta(\dot{\gamma})$ capillary. 1 = PE3, 2 = PE1, 3 = PA6, and 4 = PE4.

to be spherical. At high shear stress [Fig. 3(b)], the particles are ellipsoidal. In the extensional flow, the drops are deformed to ellipsoids and are aligned in the direction of the flow. The deformation increases with increasing draw ratio D_R ($=V_R/V_E$). This is illustrated in Figures 4 and 5.

The effects of an interfacial agent are a reduction in the size of the drop and a decrease in the deformation.

Further details on the sample preparation, on the analysis of deformation, and on the rheological properties of the polymers are given by Gonzalez-Nunez.[20]

MATHEMATICAL MODEL

We consider the deformation of a single drop in a flow field and assume that the drop is aligned in the direction of flow, as shown in Figure 6. We first compute the stress field in a sheet of fluid, which is being drawn downwards, as illustrated in Figure 1. Figure 1 also shows the chosen rectangular Cartesian coordinate system. Following Anturkar and Co,[21] we make the following assumptions.

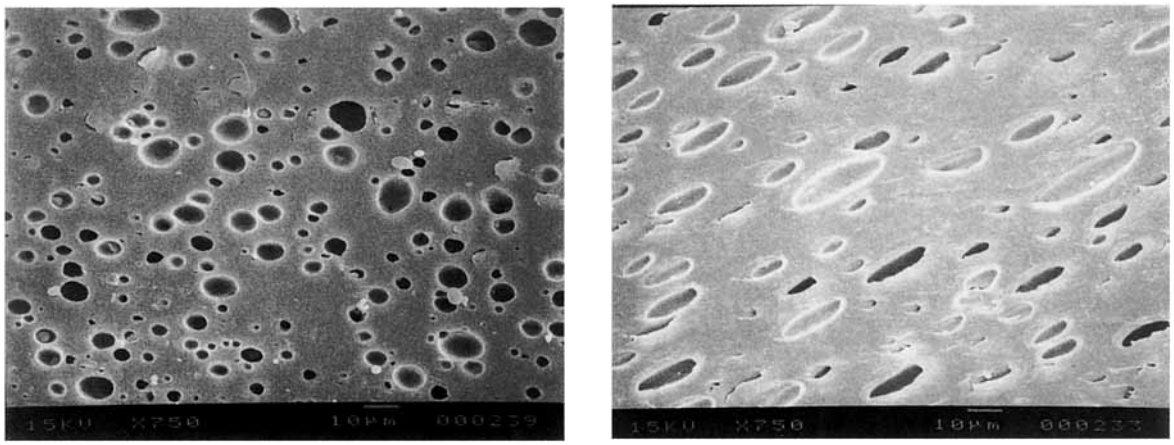

Figure 3 Deformation of the dispersed phase in a shear flow under different shear stresses τ_a: (a) τ_a = 17 kPa and (b) τ_a = 29 kPa.

1. The flow is isothermal, steady, and incompressible.
2. The extrudate swell at the exit is not considered.
3. The velocity component V_y is negligible, and V_z is a function of z only. From the equation of continuity and assuming the flow to be extensional, we deduce

$$V_x = -x\frac{dV_z}{dz} + \text{constant} \qquad (1)$$

4. The extra stress tensor $\underline{\underline{\tau}}$ is a function of z only.
5. Fluid inertia, gravity, surface tension, and air drag are neglected.
6. The sheet is plane. Combining assumptions (4) and (5) yields

$$\tau_{xx} = -P \qquad (2)$$

where P is the isotropic pressure.

7. The constitutive equation used is

$$\underline{\underline{\tau}} + \lambda_M(\dot{\gamma})\overset{\nabla}{\underline{\underline{\tau}}} = -\eta_M(\dot{\gamma})\underline{\underline{\dot{\gamma}}} \qquad (3a)$$

$$\overset{\nabla}{\underline{\underline{\tau}}} = \frac{\partial \underline{\underline{\tau}}}{\partial \tau} + \underline{V}\cdot\underline{\nabla}\underline{\underline{\tau}} - \underline{\underline{\tau}} \cdot \underline{\nabla V} - (\underline{\nabla V})^{\dagger}\cdot\underline{\underline{\tau}} \qquad (3b)$$

where $\underline{\underline{\dot{\gamma}}}$ is the rate-of-strain tensor, λ_M and η_M are the relaxation and viscosity functions, $\dot{\gamma}$ is the second invariant of $\underline{\underline{\dot{\gamma}}}$, and † denotes the transpose.

We introduce the following dimensionless quantities.

$$\phi = V_Z/V_E, \quad T_{ij} = \tau_{ij}L/(\eta_O V_E), \quad \Lambda = \lambda_M/\lambda_O \qquad (4a\text{–}c)$$

$$H = A_z/A_O = h(z)/h_O, \quad T_O = \mathrm{FL}/(\eta_O V_E A_O), \quad \zeta = z/L \qquad (4d\text{–}g)$$

$$\chi = x/L, \quad De = \lambda_M V_O/L, \quad \eta = \eta_M/\eta_O \qquad (4h\text{–}j)$$

where A_z and $h(z)$ are the area and thickness of the sheet at position z; η_O, λ_O are constants, and F is the tensile stress acting on the sheet.

The relevant components of the constitutive equation, the balance of mass and momentum, are given respectively by

$$T_{\zeta\zeta} + \Lambda De\left[\phi\frac{dT_{\zeta\zeta}}{d\zeta} - 2T_{\zeta\zeta}\frac{d\phi}{d\zeta}\right] = -2\eta\frac{d\phi}{d\zeta} \qquad (5a)$$

$$T_{\chi\chi} + \Lambda De\left[\phi\frac{dT_{\chi\chi}}{d\zeta} + 2T_{\chi\chi}\frac{d\phi}{d\zeta}\right] = 2\eta\frac{d\phi}{d\zeta} \qquad (5b)$$

$$\frac{d}{d\zeta}[\phi H] = 0 \qquad (6)$$

$$\frac{d}{d\zeta}[(T_{\zeta\zeta} - T_{\chi\chi})H] = 0 \qquad (7)$$

The boundary conditions are

$$H(0) = 1, \quad \phi(0) = 1, \quad \phi(1) = D_R \qquad (8a\text{–}c)$$

On integrating eq. (6) and using eq. (8a,b), we obtain

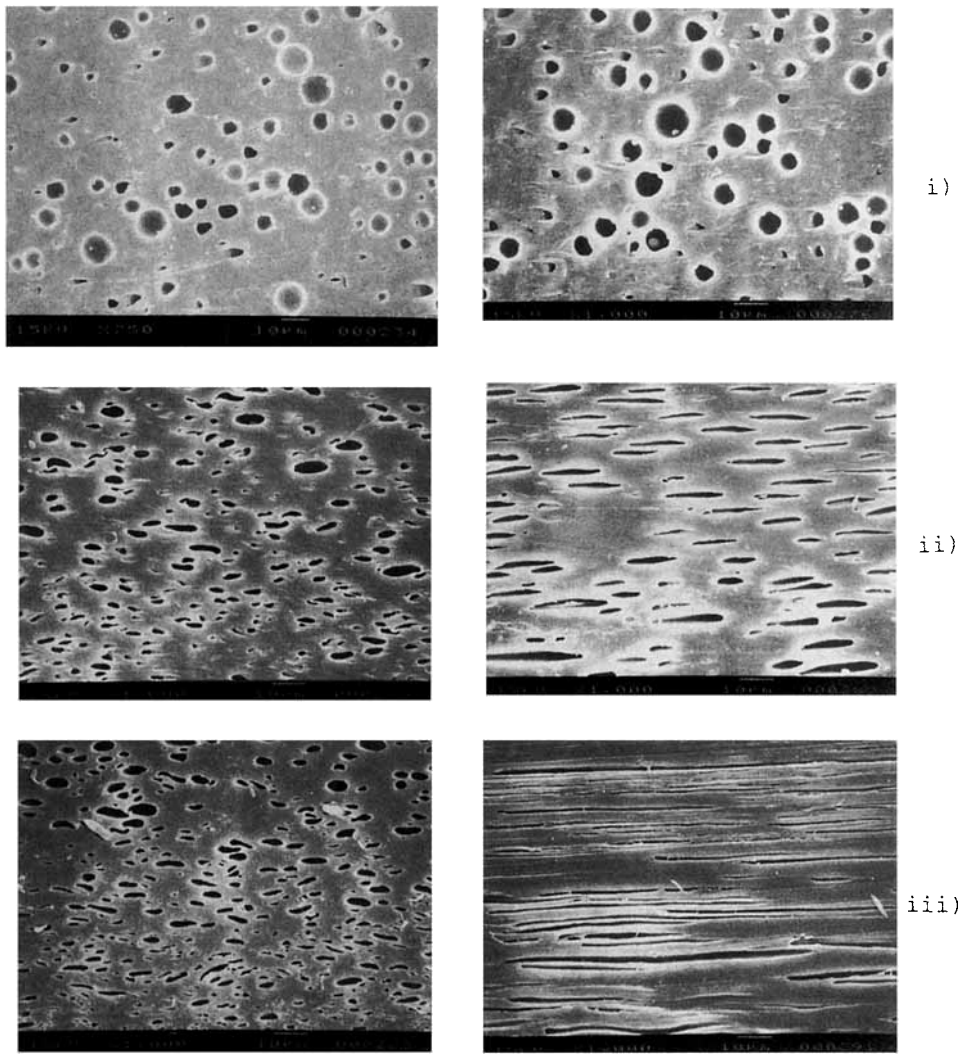

Figure 4 Deformation of the dispersed phase in a blend of 20 vol % of PA6 in PE1 without interfacial agent as a function of D_R: (i) D_R = 1.0, (ii) D_R = 2.82, and (iii) D_R = 3.97; (a) transversal section, (b) longitudinal section.

$$\phi H = 1 \tag{9}$$

Equation (7) can be integrated, and imposing the condition given by eq. (9) yields

$$T_{\zeta\zeta} - T_{xx} = -T_O\phi \tag{10}$$

From eqs. (5a,b and 10), we deduce an equation for ϕ, and it can be written as

$$\frac{T_O\phi^2\phi''}{4\phi'^2} + \frac{T_O\Lambda'\phi^2}{4\Lambda\phi'} - \frac{T_O\phi}{4\Lambda\phi' De} - \frac{\eta\Lambda'\phi}{\Lambda} + \frac{\eta}{\Lambda De} - \frac{T_O\phi}{2} + \frac{3}{4}T_O\Lambda\phi\phi' De + \eta'\phi = 0 \tag{11}$$

where the prime denotes differentiation with respect to ζ.

Equation (11) is a second-order equation, where T_O is unknown. We cannot prescribe both T_O and D_R. In our experimental setup, we control D_R, and T_O has to be adjusted so as to satisfy eq. (8c). We note that for a Newtonian fluid, eq. (11) reduces to

$$-\frac{T_O\phi}{4\phi'} + \eta = 0 \tag{12}$$

The solution of eq. (12) subject to condition (8b) is

$$\phi = \exp[T_O\zeta/(4\eta)] \tag{13}$$

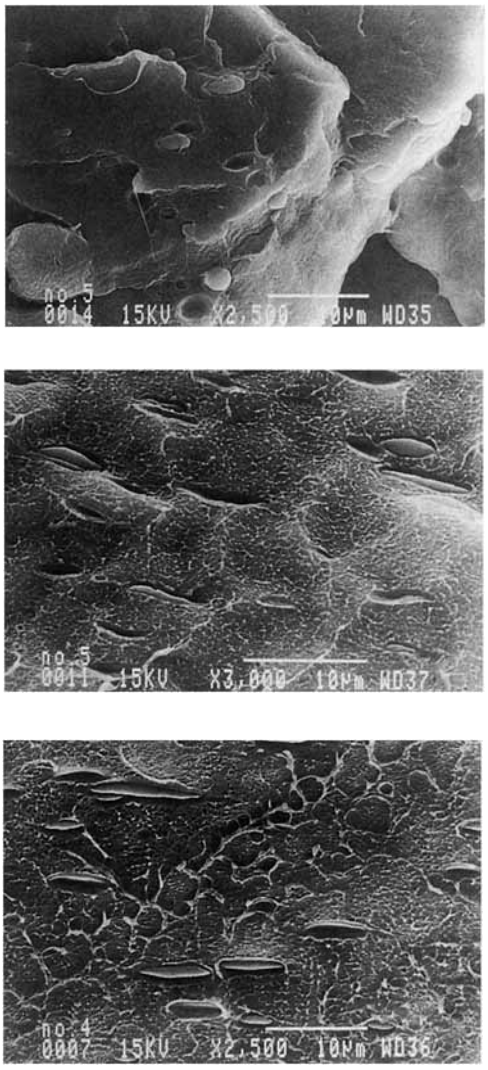

Figure 5 Deformation of the dispersed phase in a mixture of 1 vol % of PA6 in PE1 without interfacial agent for (a) $D_R = 1.0$, (b) $D_R = 2.34$, and (c) $D_R = 3.75$.

The relationship between T_O and D_R for a Newtonian fluid is

$$T_O = 4\eta \ln D_R \tag{14}$$

For a viscoelastic fluid, eq. (11) is of second order, and we need to impose an additional boundary condition. Following Denn et al.,[22] Anturkar and Co,[21] and Agassant et al.,[23] we impose the condition

$$T_{\zeta\zeta}(0) = \tau_O \tag{15}$$

Equation (15) can also be interpreted as a condition on $\phi'(0)$; and from eqs. (5a,b) and (10), we deduce

$$\tau_O = \frac{\eta}{\Lambda De} - \frac{3}{4}T_O - \frac{T_O}{4\Lambda De\phi'(0)} \tag{16}$$

For a Newtonian fluid we obtain from eqs. (5a) and (13)

$$\tau_O = -T_O/2 \tag{17}$$

Equation (11) is solved by the method of matched asymptotic expansions, and the solution to order De^2 is

$$\begin{aligned}\phi = &\left[1 - \frac{T_O De}{4} + \frac{T_O De^2 \tau_O}{4}\right]\exp(T_O\zeta/4) \\ &+ \frac{T_O De}{4}\left[1 + \frac{T_O De}{4}\right]\exp(T_O\zeta/2) \\ &+ \frac{De^2 T_O^2}{16}\exp(3T_O\zeta/4) - \frac{De^2 T_O^2}{4} \\ &\times\left[\frac{\tau_O}{T_O} + \frac{1}{2}\right]\exp(-\zeta/De) + O(De^3)\end{aligned} \tag{18}$$

A numerical solution, using the Runge Kutta method, is also obtained. We have verified that for low values of De ($De < 0.1$), the numerical and asymptotic solutions are in agreement. Further details on both methods are available in Gonzalez-Nunez.[20] Once ϕ has been computed, the stress components can be calculated.

Figure 7 shows the values of $T_{\zeta\zeta}$ for various values of De and for $D_R = 4.33$. The magnitude of $T_{\zeta\zeta}$ increases with increasing De. Figure 8 illustrates the values of $T_{\zeta\zeta}$ (1) as a function of D_R. As expected, for low values of D_R, the effect of elasticity is negligible. The total axial stress $\pi_{\zeta\zeta}$ [$=p + T_{\zeta\zeta} = T_{\zeta\zeta} - T_{xx}$] at $\zeta = 1$ as a function of D_R is shown in Figure 9. For low values of D_R, the values of $\pi_{\zeta\zeta}$ (1) for both Newtonian and viscoelastic fluids are almost equal.

We now calculate the deformation that a spherical drop undergoes when placed in a stress field. We consider an isolated single drop and, as a first ap-

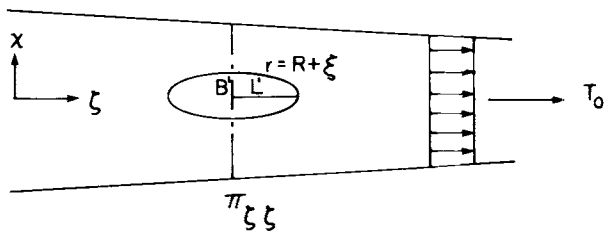

Figure 6 Deformation of a single drop in an elongational flow.

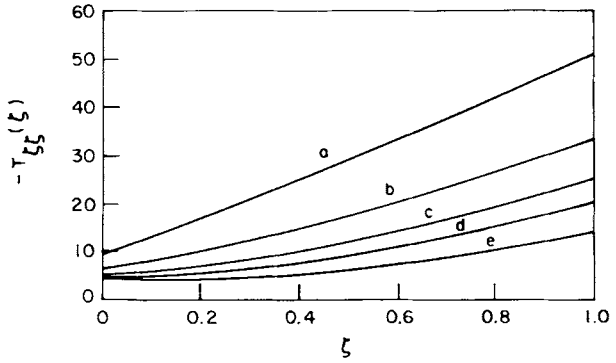

Figure 7 Axial stress as a function of ζ for various values of De: (a) $De = 0.25$, (b) $De = 0.20$, (c) $De = 0.15$, (d) $De = 0.10$, and (e) $De = 0.01$. $D_R = 4.33$.

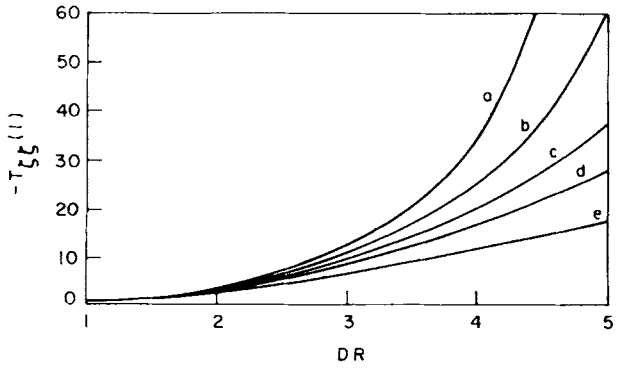

Figure 8 Axial stress at $\zeta = 1$ as a function of D_R for the same values of De as in Figure 6.

proximation, we assume that the presence of the drop does not affect the elongational flow field. Subscripts m and d are used to designate the matrix and the dispersed phase, respectively. The boundary conditions at the interface are as follows:

$$\phi_m = \phi_d \tag{19}$$

$$\left(\underline{\underline{\pi}}_m - \frac{\eta_d}{\eta_m}\underline{\underline{\pi}}_d\right)\cdot \underline{n} = \mathrm{Ca}\, k\, \underline{n} \tag{20}$$

where $\underline{n}$ is the unit outward normal, k is the surface curvature, and Ca is the capillary number. Choosing the center of the drop as the origin of a spherical polar coordinate system (r, θ, ϕ), the radial distance r of any point on the surface can be written as

$$r = R + \xi \tag{21}$$

where R is the radius of the undeformed drop.

For a cross section of the drop (ϕ = constant) and for small deformations, k can be approximated[24] as

$$k = \frac{2}{R} - \frac{2\xi}{R^2} - \frac{1}{R^2}\left[\frac{1}{\sin\theta}\frac{d}{d\theta}\left(\sin\theta\frac{d\xi}{d\theta}\right)\right] \tag{22}$$

In our experiments, the range of De is 0.01 to 0.05, and the asymptotic solution (eq. 18) is a valid solution. Transforming the calculated Cartesian components of the stress tensor into spherical coordinates, substituting into eq. (20) and using eqs. (19) and (22), we obtain

$$\frac{d^2\xi}{d\theta^2} + \cot\theta\frac{d\xi}{d\theta} + 2\xi - 2R - R^2\mathrm{Ca} \times\left(1 - \frac{\eta_d}{\eta_m}\right)T_O\exp\left[\frac{T_O}{4L}(R + \xi)\cos\theta\right] = 0 \tag{23}$$

Equation (23) is solved numerically using the Runge-Kutta method. We have imposed the conditions that at $\theta = \pi/2$,

$$\xi = R_O \quad \text{and} \quad \frac{d\xi}{d\theta} = 0 \tag{24a,b}$$

Knowing ξ, the major (L') and the minor (B') axes of the drop can be computed. It is usual to define the deformation D' as

$$D' = \frac{L' - B'}{L' + B'} \tag{25}$$

Figure 10 compares the predicted values of D' as a function of Ca with the experimental values of

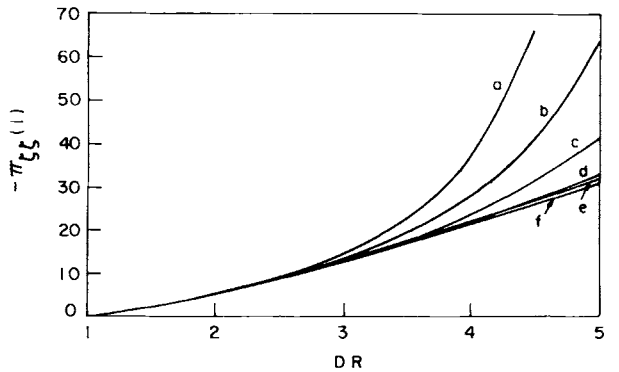

Figure 9 Total axial stress at $\zeta = 1$ as a function of D_R for the same values of De as in Figure 6 and for a Newtonian fluid (f).

blends of PE1/PA6 with and without interfacial modifier. Figure 11 shows the shape of the drops for various values of Ca.

DISCUSSION

Figure 10 shows quantitative agreement between theoretical predictions and experimental results, even at high Ca, where we would not expect the small deformation approximation to be valid. Delaby et al.,[25] under a different set of conditions, observed similar results. This suggests that in calculating D', the small deformation approximation is not very severe.

The predicted shape does not agree with our experimental observations for Ca > 0.4. For Ca > 0.4, we predict a constriction at the central part of the drop, as shown in Figure 11. Experimentally, the drops are always ellipsoidal, in agreement with the findings of Delaby et al.[25] Buckmaster and Flaherty[26] have also predicted that a drop deforms into an ellipse at low values of capillary number; and as the capillary number increases, the central portion of the drop flattens. Their findings are in agreement with ours. The disagreement between our predictions and observations may be due to the fact that above a certain critical capillary number (Ca_c), the shape of the drop is time-dependent, and we have not considered time effects. Milliken and Leal[10] have observed that for $Ca > Ca_c$, the shape of a drop is time-dependent as time evolves, keeping all other variables constant. The shape changes from an ellipsoid to almost a dumbbell. Eventually the drop may break. In our experiment, the drop is subjected to a variable stress field as it is transported from the exit of the die to the roller. That is to say, its residence time at constant stress is zero. Consequently, a constriction at its central part does not develop. There may be other factors that might contribute to the discrepancy between theoretical and experimental results. The effects of the presence of other drops, of coalescence, and the perturbation on the basic extensional flow created by the drop have been ignored. These factors could contribute significantly to the shape of the drop.

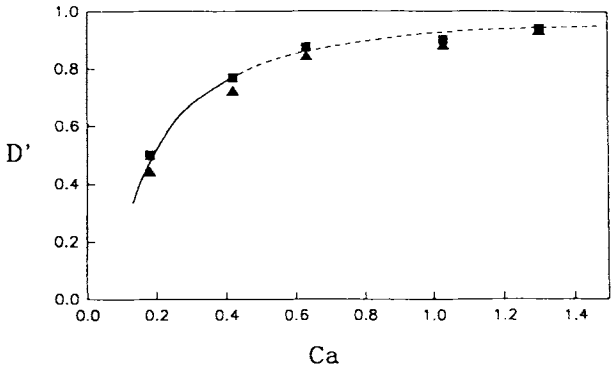

Figure 10 D' versus Ca for a mixture of PE1 and PA6: (■) PA6, 20 vol % with interfacial agent, $\eta_m/\eta_d = 1.10$; (▲) PA6, 1 vol % without interfacial agent, $\eta_m/\eta_d = 1.10$. Predictions of eq. 23: (——) agreement in both deformation and shape; (- - - -) agreement in deformation only.

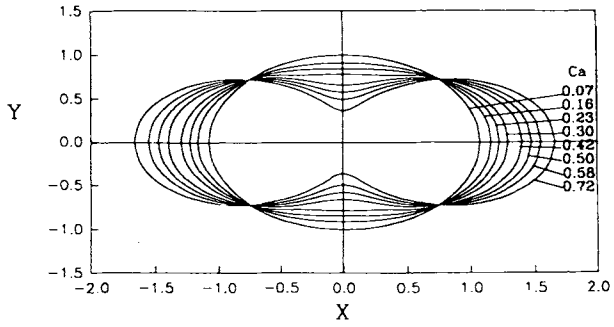

Figure 11 Shape of a drop for various values of capillary number. $\eta_m/\eta_d = 1.10$.

It is observed that the presence of an interfacial agent decreases the deformation. As shown in Figure 10, the deformation in a blend of 20 vol % PA6 in PE1 with interfacial agent is similar to that of a 1 vol % PA6 in PE1 without interfacial agent.

The present analysis has shown that the deformation D' can quantitatively be predicted, but a more careful analysis is needed to predict the shape of the deformed drop.

REFERENCES

1. B. D. Favis, *Can. J. Chem. Eng.*, **69**, 619 (1991).
2. R. J. M. Borggreve and R. J. Gaymans, *Polym.*, **30**, 63 (1989).
3. R. J. M. Borggreve, R. J. Gaymans, and J. Schnijer, *Polym.*, **30**, 71 (1989).
4. P. Van Gheluwe, B. D. Favis, and J. P. Chalifoux, *J. Mat. Sci.*, **23**, 3910 (1988).
5. G. I. Taylor, *Proc. Roy. Soc.*, **A146**, 501 (1934).
6. F. D. Rumscheidt and S. G. Mason, *J. Colloid Sci.*, **16**, 238 (1961).
7. H. B. Chin and C. D. Han, *J. Rheol.*, **23**, 557 (1979).
8. H. P. Grace, *Chem. Eng. Commun.*, **14**, 225 (1982).
9. B. J. Bentley and L. G. Leal, *J. Fluid Mech.*, **167**, 219 (1986).
10. W. J. Milliken and L. G. Leal, *J. Non-Newtonian Fluid Mech.*, **40**, 355 (1991).

11. W. J. Milliken and L. G. Leal, *J. Non-Newtonian Fluid Mech.*, **42,** 231 (1992).
12. J. M. Rallison, *Ann. Rev. Fluid Mech.*, **16,** 45 (1984).
13. H. A. Stone, *Ann. Rev. Fluid Mech.*, **26,** 65 (1994).
14. M. V. Tsebrenko, G. P. Danilova, and A. Y.-A. Malkin, *J. Non-Newtonian Fluid Mech.*, **31,** 1 (1989).
15. M. J. Milliken, H. A. Stone, and L. G. Leal, *Phys. Fluids,* **A5,** 69 (1993).
16. M. J. Milliken and L. G. Leal, *J. Colloid Interf. Sci.*, **166,** 275 (1994).
17. J. M. Willis, V. Caldas, and B. D. Favis, *J. Mat. Sci.*, **26,** 4742 (1991).
18. J. M. Willis, B. D. Favis, and C. Lavallée, *J. Mat. Sci.*, **28,** 1749 (1993).
19. S. A. Saltikov, *Stereometric Metallography,* 2nd ed., Metallurgizdat, Moscow, 1958.
20. R. Gonzalez-Nunez, Ph.D. thesis, University of Sherbrooke, Sherbrooke, Quebec, Canada (1994).
21. N. R. Anturkar and A. Co, *J. Non-Newtonian Fluid Mech.*, **28,** 287 (1988).
22. M. M. Denn, C. J. S. Petrie, and P. Avenas, *AIChE. J.*, **21**(4), 791 (1975).
23. J. F. Agassant, P. Saillard, and B. Vergnes, *Rev. Gén. Therm. Fr.*, **477,** 272 (1984).
24. L. D. Landau and E. M. Lifshitz, *Fluid Mechanics,* Pergamon, New York, 1987.
25. I. Delaby, B. Ernst, Y. Germain, and R. Muller, *J. Rheol.*, **38**(b), 1705 (1994).
26. J. D. Buckmaster and J. E. Flaherty, *J. Fluid Mech.*, **60**(4), 625 (1973).

Received August 29, 1995
Accepted June 10, 1996